Colloid and Interface Science Communications 19 (2017) 31–34

Contents lists available at ScienceDirect

Colloid and Interface Science Communications

journal homepage: www.elsevier.com/locate/colcom

Synthesis of Gadolinium-based Nanostructures Through an Enzymatic Liposome-controlled Reaction

Sofía Municoy*, Martín G. Bellino

Departamento de Micro y Nanotecnología, Comisión Nacional de Energía Atómica, Av. Gral Paz 1499, B1650KNA San Martín, Buenos Aires, Argentina

ARTICLE INFO

Keywords:
Liposome
Urease
Biomineralization
Gadolinium-based nanostructures
Enzymatic-controlled reaction

ABSTRACT

The success of synthesis of varied nanostructures requires the precise precipitation of materials at particular location. Here, gadolinium carbonate nanocapsules or macroporous structures have been successfully synthesized via interplay control on enzymatic precipitation and liposome templating. The nanostructures reflected the shape of the liposomes, where spherical 560 nm size and porous architectures with large pores of 200–300 nm diameter (corresponding to sections along liposomes) ensembles were formed. The manipulation over location of ureases in the liposome system and the temperature-actuated vesicle permeability were crucial factors in determining the morphology of the final product. This liposome-directed enzymatic precipitation represents a powerful yet facile method for lanthanide-based nanostructures synthesis for promising applications.

The generation of new approaches that enable bio-control of nucleation and growth of materials continues to be an expanding and challenging field of research. This research is driven by the promise that control of biomineralization can significantly impact areas as diverse as novel material synthesis methods and biological process understanding. Biological systems utilize diverse biomacromolecules (proteins, polysaccharides and lipids) to modulate the formation of inorganic minerals [1]. In this sense, various enzymes, such as alkaline phosphatase, carbonic anhydrase, silicatein and urease, play crucial roles in synthesis and growth of biominerals. To date, extensive techniques have been developed for mimicking nature generally relying on urease-catalyzed hydrolysis of urea to prompt carbonate precipitation [2,3]. Successful strategies for enzymatic formation of monodispersed particles of different composition, such as calcium carbonates [4] and rare-earth oxides [5,6] are widely reported; however, interplay of control on enzymatic precipitation and biological membrane templating is significantly more challenging. This is due to the more demanding requirements to develop intricate structures mimicking nature. The presence of organic matrices during the biomineralization process acts as inert templates that allows a controlled growth of the inorganic material due to their complementarity with the surface structure, charge and geometric configuration [7]. While lipid vesicles (liposomes) have been widely employed for numerous biomedical and industrial applications [8,9,10,11], in particular, liposomes have been used for the development of different biomineralization processes [12], in which they act as a template for the precipitation of different inorganic compounds, such as calcium carbonate [1,13] and phosphate [14] or gadolinium hydroxide [15]. All of these liposome precipitation strategies mentioned above involve inert templates with no evidence of liposome influence on the control of an enzymatic-based precipitation. As a novel approach, a liposome-actuated enzymatic precipitation principle to generate liposomes encapsulated in a silica shell was recently reported [16]. The synergic interplay between enzymes and liposomes that mimicking crucial aspects of cellular biochemistry such as confinement and enzymatic regulation, leads to a partial dissolution of a sacrificial mesoporous silica film and bio-active reconstruction of a fully 3D silica shell around liposomes. Herein, an extension of this original liposome-directed enzymatic precipitation (LDEP) approach is described in order to illustrate that nanostructures of gadolinium-based compounds can indeed be prepared by the LDEP strategy. Advantages to this new approach include: (i) lanthanide compounds have promising applications, e.g., cancer radiotherapy [17], in vivo imaging [18] and neuroprotection [19]; (ii) in particularly, gadolinium, the most abundant element in the lanthanide family, has tremendous importance as nuclear, electronic, laser, optical, catalyst and phosphor material [20,21]; (iii) control over location of enzymes in the liposome system allows to produce a diversity of nanoarchitectures; (iv) memory of the original structure of the liposomes into the biomineralized nanomaterials is achieved. This report focuses on the general characteristics of the synthesized nanomaterials and the mechanisms that govern these nanostructures formation.

Strategies for precipitation of gadolinium carbonate from water are well known and frequently applied. Urea appears as a source of the carbonate ions, which is specifically advantageous to obtain well-

* Corresponding author.
E-mail address: municoy@cnea.gov.ar (S. Municoy).

http://dx.doi.org/10.1016/j.colcom.2017.07.002
Received 2 June 2017; Received in revised form 10 July 2017; Accepted 14 July 2017

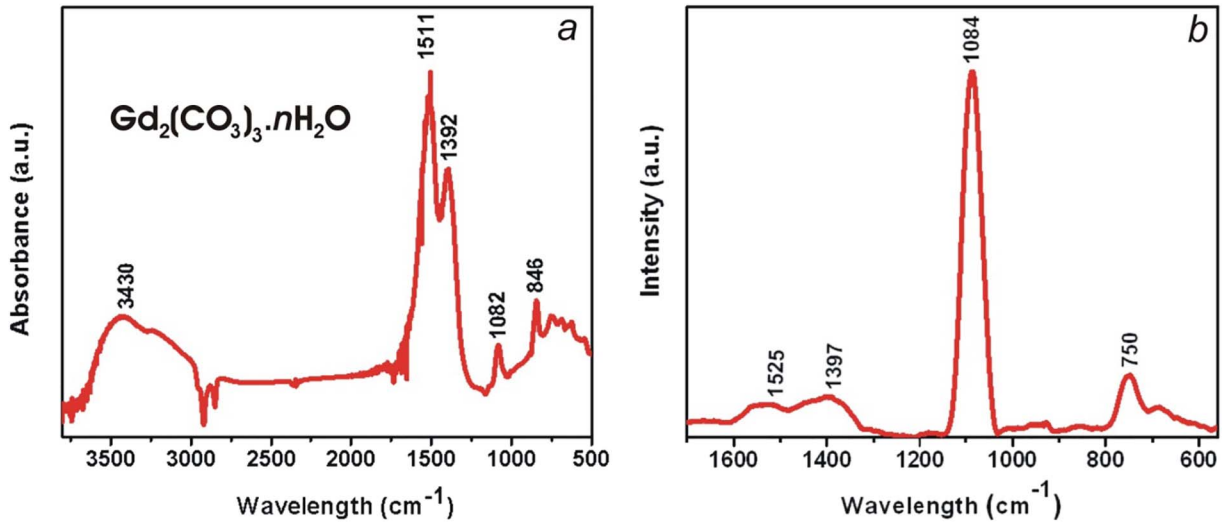

Fig. 1. FTIR (a) and Raman (b) spectra of gadolinium carbonate precipitates.

defined particles [22,23]. Gadolinium reacts with urea to form a complex $[Gd(urea)_3](NO_3)_3$. In presence of urease, urea breaks down and gadolinium carbonate precipitates through the following reaction:

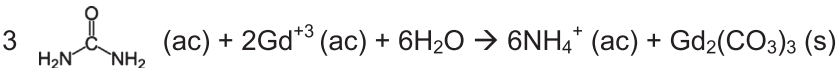

With this in mind, firstly, gadolinium carbonate precipitates were prepared via urease-catalyzed hydrolysis of urea. Briefly, a solution containing urea 0.5 M and urease 0.1 mg/ml (Jack bean) was mixed with $Gd(NO_3)_3$ 0.05 M at 25 °C and 45 °C and the precipitate formed was then separated by centrifugation, washed and re-suspended in water. As a result, a similar precipitate formed by the agglomeration of small nanoparticles was obtained at both temperatures studied (see Fig. S1 in Supplementary information). Fourier Transform Infrared (FTIR) and Raman spectroscopy were then performed to characterize the composition and structure of the precipitates. Fig. 1a shows a typical FTIR spectrum taken from dry powders of as-obtained precipitates.The intense bands between 1300 and 1500 cm^{-1} can be attributed to the asymmetric stretching vibration of C═O bond, while the C—O stretching peak appears at 1082 cm^{-1} and the band at 846 cm^{-1} can be assigned to the CO_3^{-2} wagging mode [24]. In Raman spectrum (Fig. 1b), CO_3^{-2} symmetric stretching mode appears intensely at 1084 cm^{-1}, while CO asymmetric stretching bands and CO_3^{-2} bending modes can be observed with low intensity at 1300–1600 cm^{-1} and 750 cm^{-1}, respectively [25]. These results lead to the conclusion that the precipitates are composed of $Gd_2(CO_3)_3$.

The use of liposomes as templates for gadolinium-based deposition implies a non-trivial approaches since these template structures are sensitive to pH and ionic strength. For these reasons, an experimental design previously reported based on the preparation of equivalent systems containing the same liposome and enzyme concentration was used. Gadolinium precipitation on the bilayer surface is expected to be favorable since the concentration of gadolinium ions near the interface is high due to electrostatic interactions, because positive charged Gd species are attracted by the mildly negative DPPC lipids. In fact, it was demonstrated that the z-potential value increases from − 4 mV for the lipid template vesicles of DPPC/Cholesterol to + 42 mV for the gadolinium/liposome solutions. In a typical synthesis, liposome solution was prepared with DPPC/Cholesterol 1:0.2 by the lipid film hydration and extrusion method. As reported before, the vesicles exhibit a gel-to-liquid crystalline phase transition at temperature (Tm) of 40 °C [15] and dynamic light scattering (DLS) measures show the typical averaged diameter of 410 nm (Fig. S2). Urease/Liposome System section in Supplementary Information illustrates the experimental design, where platforms composed of liposomes and free ureases (active + denaturalized) with the same activity at T < Tm (25 °C) and T > Tm (45 °C) (named LF25 and LF45 respectively), were compared to equivalent assemblies of liposomes entrapping ureases (labeled LE25 and LE45), hereafter, the tags denoting the synthesis temperature. The vesicle/enzyme systems were set to a pH of 5 by gentle addition of diluted HCl aliquots, prior to the addition of the gadolinium salt ($Gd(NO_3)_3$0.5 M) and urea 0.5 M. After that, the solution was stirred for 60 min at 25 °C or 45 °C, and subsequently was centrifuged at 6000 rpm for 30 min.

SEM images clearly indicate that the vesicles in the LE25 system are, indeed, completely covered by precipitated gadolinium carbonate (Fig. 2a), since bare vesicles would entirely disintegrate upon dehydration and as a consequence become “invisible” in SEM. In this case, uniform spheres with an average diameter of 560 nm were obtained, in close comparison with the starting liposomes. According to these results, TEM and SEM images of the precipitated product and the DLS measurement of the lipid vesicles indicate a gadolinium-based wall thickness of about 75 nm. Their thickness is thin enough to be partially transparent to the electron beam (Fig. 3a). However, no evidence of coated vesicles could be found in the LE45 system. All micrographs indicate the production of small particles of different size and morphology with a typical size of about 100 to 500 nm (Figs. 2b and 3b). Morphological changes are obvious, as the typical spherical shape of the LE25 precipitates has disappeared. Apparently, the LE45 system is not sufficiently stable to achieve heterogeneous precipitation surrounding liposomes. It is anticipated that this different behavior is closely related to the liposome membrane permeability.

When looking at the TEM and SEM pictures of LF25 and LF45 systems, Fig. 2c and d, one can observe interesting and peculiar morphologies: porous matrices with pores of different sizes (mainly with diameters in the 200–300 nm range, see Fig. S5 in SI). Remarkably, precipitation and templating reactions were also conducted for vesicle solutions.These pores, however, were better defined in LF25 than in LF45 because the stability of vesicles at 45 °C is lower than that at 25 °C (see Fig. 3c and d). When realizing that the bilayer behavior of vesicles is close to fluid-like at 45 °C, whereas for 25 °C it is still gel-like, it becomes plausible that vesicles at 45 °C are failing to act as template

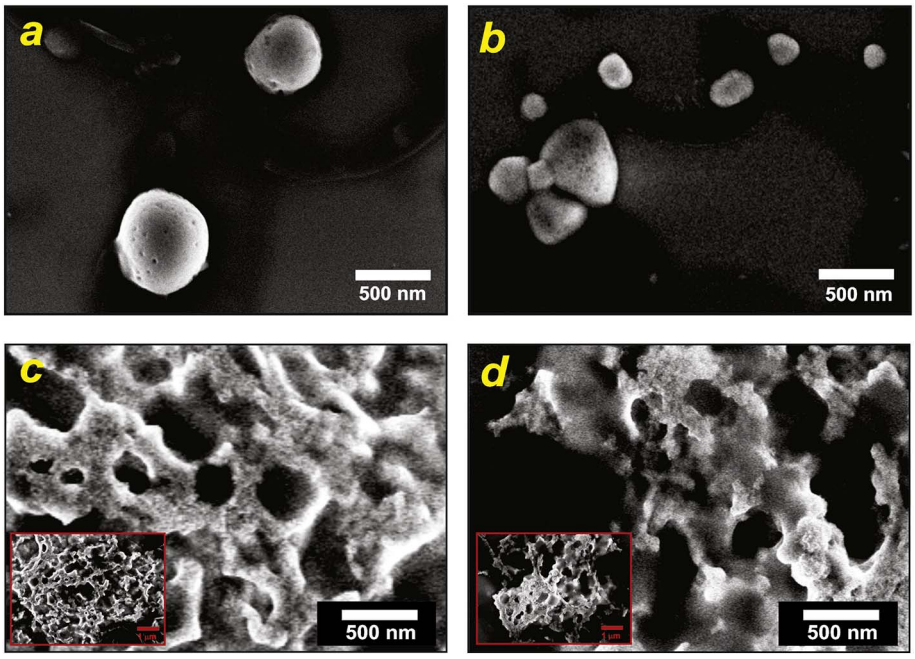

Fig. 2. SEM images of the gadolinium carbonate structures obtained via urease-catalyzed hydrolysis of urea at 25 °C (a and c) and 45 °C (b and d), from a solution containing gadolinium nitrate 0.5 M, urea 0.5 M and encapsulated (a and b) or free (c and d) urease/liposome system. The insets in c and d show a general view of the porous nanostructures.

for gadolinium precipitation.

Clearly, the location of enzymes in the liposome systems (free or encapsulated) affects the morphology of the precipitates. In the case of the liposome encapsulating ureases, the paradigm that templating demands a limited urea permeability through the lipid bilayer ($T < Tm$) and, of course, structural and mechanical stability of the template was illustrated. This limitation leads to slow down urea degradation by the encapsulated urease, producing then a minor quantity of carbonate ions that permeate through the membranes and react with gadolinium adsorbed on the liposomes surface. In this case, the lipid membranes act as nucleation centers for the formation of the inorganic coating, obtaining finally hollow spherical particles (see Fig. 4a). However, when $T > Tm$, the permeability of the membranes increases and the reaction rate is higher, so the carbonate ions leave the liposomes quickly and diffuse throughout the solution. Because of that and due to the greater mobility of the lipid bilayer the gadolinium precipitation does not necessarily occur on the surface of the liposomes, resulting in the formation of a wide variety of structures of different morphologies and sizes across the solution (see Fig. 4b). In contrast, no activation and inhibition of enzyme activity by a change of the lipid bilayer permeability through temperature for the free urease system leads to obtain similar porous structures at both 25 and 45 °C temperatures. The presence of multiple pores indicates that precipitation occurred homogenously in the solution and eventually heterogeneously on the surface of the liposomes, which were simultaneously trapped by the precipitated structure. The different diameters of the cavities suggest that the precipitation happened in various sections along the liposomes, as shown in Fig. 4c and d.

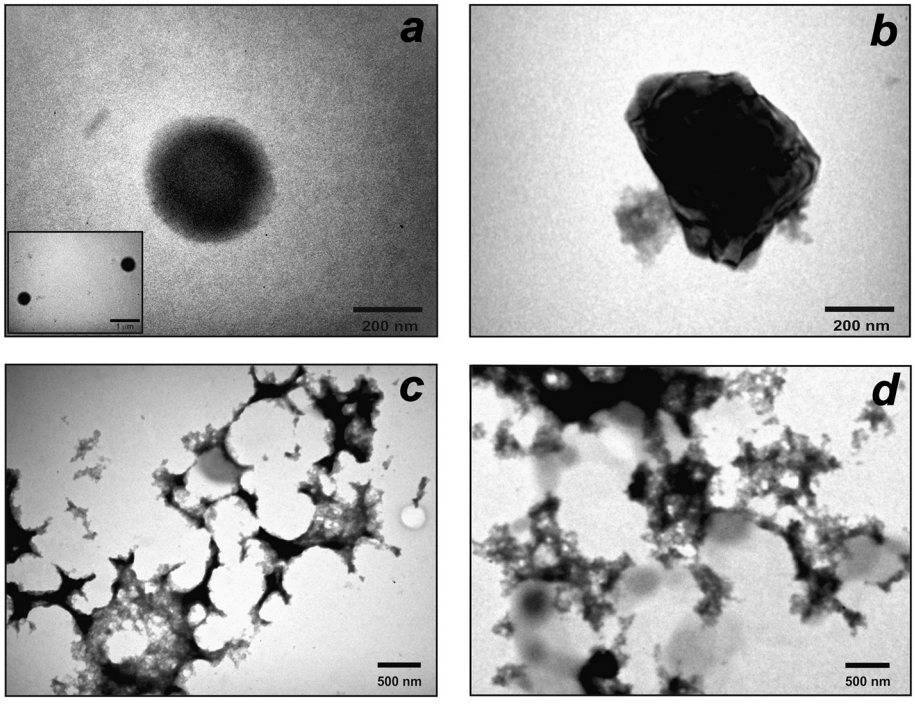

Fig. 3. TEM images of the gadolinium carbonate structures obtained via urease-catalyzed hydrolysis of urea at 25 °C (a and c) and 45 °C (b and d), from a solution containing gadolinium nitrate 0.5 M, urea 0.5 M and encapsulated (a and b) or free (c and d) urease/liposome system.

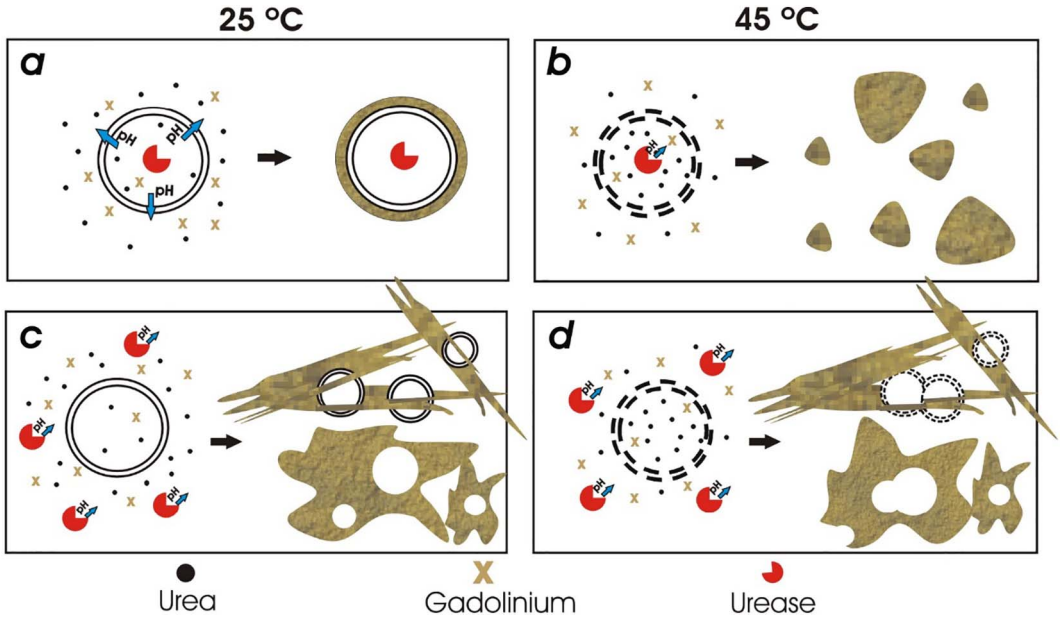

Fig. 4. Representative scheme of the proposed gadolinium precipitation mechanism for the studied systems.

In summary, here an enzymatic-liposome route to a large-scale synthesis of gadolinium-based nanostructures was described. These structures emerge from the ability of liposome entrapping ureases system at T < Tm to actively develop a favorable pH gradient through the lipid interface that catalyzes gadolinium precipitation within a three-dimensional volume surrounding the liposome. Porous matrices with a liposome-templated porosity were also generated by positioning the enzymes outside the vesicles. This liposome-directed porosity was attributed to a transcription of the vesicle in an imprinting into the precipitates during the course of the enzymatic homogeneous precipitation. The principle of liposome-actuated enzymatic activity and controlled position enzyme/liposome assembly were key to obtaining dissimilar precipitated nanostructures. These mutual liposome/enzyme interactions during the precipitation process, as well as their combined influence on the morphological evolution of the total system open the way for finally arrive at a construction tool-kit for novel lanthanide-based nanostructures. Because of their electrical, magnetic, optical and nuclear properties, these structures are promising for many applications, such as in catalysts, medical diagnostics, lasers, semiconductors, nuclear fuel elements, phosphors, and glass polishers.

Acknowledgements

This work was supported by ANPCyT (PICT 2969). SM acknowledges CONICET for a doctoral scholarship. We thank to G. Zbihlei of Lab. de Microscopía Electrónica-Gerencia Materiales-CNEA for TEM images. We thank Dr. A. Wolosiuk for assistance with DLS technique and Dra. G. Leyva for FTIR and DSC measurements.

Appendix A. Supplementary data

Supplementary data to this article can be found online at http://dx.doi.org/10.1016/j.colcom.2017.07.002.

References

[1] P. Wan, Y. Zhao, H. Tong, Z. Yang, Z. Zhu, X. Shen, J. Hu, Mater. Sci. Eng. C 29 (2009) 222–227.
[2] I. Sondi, B. Salopek-Sondi, Langmuir 21 (2005) 8876–8882.
[3] E. Hemmer, T. Yamano, H. Kishimoto, N. Venkatachalam, H. Hyodo, K. Soga, Acta Biomater. 9 (2013) 4734–4743.
[4] I. Sondi, E. Matijevic, J. Colloid Interface Sci. 238 (2001) 208–214.
[5] M. Kawashita, Y. Takayama, T. Kokubo, G.H. Takaoka, N. Araki, M. Hiraoka, J. Am. Ceram. Soc. 89 (2006) 1347–1351.
[6] N. Venkatachalam, Y. Saito, K. Soga, J. Am. Ceram. Soc. 92 (2009) 1006–1010.
[7] A. Szcześ, Colloids Surf. B: Biointerfaces 101 (2013) 44–48.
[8] L. Sercombe, T. Veerati, F. Moheimani, S.Y. Wu, A.K. Sood, S. Hua, Front. Pharmacol. 6 (2015) 286.
[9] Y. Liu, J. Liu, Langmuir 32 (2016) 13276–13283.
[10] E. Khanniri, N. Bagheripoor-Fallah, S. Sohrabvandi, A.M. Mortazavian, K. Khosravi-Darani, R. Mohammad, Crit. Rev. Food Sci. Nutr. 56 (2016) 484–493.
[11] K.A. Edwards, Liposomes Anal. Methodol. (2016) 1–82.
[12] E.E. Golub, Biochim. Biophys. Acta Gen. Subj. 1790 (2009) 1592–1598.
[13] J. Xiao, Z. Wang, Y. Tang, S. Yang, Langmuir 26 (2010) 4977–4983.
[14] Y. Fukui, K. Fujimoto, Chem. Mater. 23 (2011) 4701–4708.
[15] S. Municoy, M.G. Bellino, ChemistrySelect 1 (2016) 723–727.
[16] S. Municoy, M.G. Bellino, RSC Adv. 7 (2017).
[17] M. Hamoudeh, M.A. Kamleh, R. Diab, H. Fessi, Adv. Drug Deliv. Rev. 60 (2008) 1329–1346.
[18] S.F. Lim, R. Riehn, W.S. Ryu, N. Khanarian, C. Tung, D. Tank, R.H. Austin, Nano Lett. 6 (2006) 169–174.
[19] D. Schubert, R. Dargusch, J. Raitano, S.-W. Chan, Biochem. Biophys. Res. Commun. 342 (2006) 86–91.
[20] R. Manigandan, K. Giribabu, R. Suresh, L. Vijayalakshmi, A. Stephen, V. Narayanan, Mater. Res. Bull. 48 (2013) 4210–4215.
[21] A. Strasser, A. Vogler, Inorg. Chim. Acta 357 (2004) 2345–2348.
[22] S. Lechevallier, P. Lecante, R. Mauricot, H. Dexpert, J. Dexpert-Ghys, H.K. Kong, G.L. Law, K.L. Wong, Chem. Mater. 22 (2010) 6153–6161.
[23] G. Accardo, L. Spiridigliozzi, R. Cioffi, C. Ferone, E. Di Bartolomeo, S.P. Yoon, G. Dell'Agli, Mater. Chem. Phys. 187 (2017) 149–155.
[24] O.B. Ibrahim, J. Chem. Pharm. Res. 4 (2012) 1036–1041.
[25] R.L. Frost, A. López, R. Scholz, Y. Xi, F.M. Belotti, J. Mol. Struct. 1051 (2013) 221–225.